JOURNAL OF GEOPHYSICAL RESEARCH, VOL. 102, NO. D25, PAGES 30,107–30,117, DECEMBER 27, 1997

Effect of black carbon and sulfate aerosols on the Global Radiation Budget

Ingrid Schult and Johann Feichter

Max Planck Institute for Meteorology, Hamburg, Germany

William F. Cooke

Environment Institute, Joint Research Center, Ispra, Italy

Abstract. Global fields of radiative forcing due to natural and anthropogenic sulfate aerosols, black carbon aerosols, and an external mixture of the two have been calculated with a one-dimensional radiative transfer model developed for estimates of the direct radiative forcing by aerosols. Estimates of solar radiative forcing by different aerosols are presented for January and July, based on calculated three-dimensional, global distributions of sulfate and black carbon mass. We show that the radiative forcing by sulfate is negative, as already known, while the forcing due to black carbon aerosols is mainly positive. Considering both black carbon and sulfate together and assuming an external mixture, we calculate a globally averaged radiative forcing of approximately -0.2 W/m^2, with a quite nonuniform geographical distribution. The radiative forcing due to aerosols is highly dependent upon the optical properties of the aerosol, while the surface reflectance and the Sun angle influence the direction of the forcing. Our results show that the presence of black carbon, the main absorbing component of anthropogenic aerosol, may reduce the cooling effect of aerosol, thus leading to an increase in the greenhouse warming.

Introduction

In recent years there has been a growing awareness that in addition to the influence of the greenhouse gases on the warming of the Earth's atmosphere, aerosol particles may also play an important role in forcing climate change [e.g., *Grassl*, 1988; *Charlson et al.*, 1991; *Intergovernmental Panel on Climate Change (IPCC)*, 1992]. Aerosols exert a direct effect on climate primarily through their interaction with solar radiation and, to a lesser degree, through their interaction with infrared radiation. Nonabsorbing aerosols will scatter more sunlight back into space, thus reducing the amount of solar radiation reaching the surface. Aerosols which absorb solar radiation, cause a warming of the absorbing atmospheric layer and a cooling of the underlying surface. The heated aerosol layer can reemit the energy in the infrared. Whether the total effect results in a net cooling or warming of the Earth-atmosphere system depends on the balance between the absorption efficiency in the visible and the infrared, the vertical distribution of aerosol, the surface albedo, the Sun elevation, and the degree of cloudiness [*Charlock et al.*, 1993].

Anthropogenic aerosol sources have increased significantly over the past century mainly due to fossil fuel use and biomass burning. The principal contributors to aerosol radiative forcing produced from these anthropogenic sources are believed to be black carbon and sulfate particles [*Charlson and Heintzenberg*, 1995]. About 40% of the global black carbon emission is estimated to arise from combustion of biomass and the other 60% from fossil fuel combustion [*Cooke and Wilson*, 1996]. The anthropogenic emissions of precursor substances for sulfate aerosols amount to about 70-80 % of the total sources of non-sea-salt sulfate. As 50-70 % of the total mass of particles is sulfate [*Kondratyev et al.*, 1983; *Weiss and Waggoner*, 1982], it is one of the main contributors to aerosol forcing. Whereas sulfate particles mainly scatter solar radiation, black carbon particles scatter and absorb and may therefore reduce the cooling by sulfate aerosols, at least over regions with high surface albedo.

Recent estimates of the direct forcing of anthropogenic sulfate aerosols range from -0.3 W/m^2 [*Kiehl and Briegleb*, 1993], -0.6 W/m^2 [*Charlson et al.*, 1991], and -0.9 W/m^2 [*Taylor and Penner*, 1994]. The estimates differ mainly due to the treatment of the effects of humidity and to the use of different extinction coefficients. *Penner et al.* [1992] estimated the direct aerosol forcing due to biomass burning for purely scattering particles to be -1.0 W/m^2 and the forcing due to absorption to be 0.2 W/m^2. *Haywood and Shine* [1995] calculated a global mean forcing due to soot and sulfate particles between -0.10 and -0.28 W/m^2. This estimate is based on the sulfate distribution by *Langner and Rodhe* [1991] assuming a constant soot/sulfate ratio.

We will present distributions of the black carbon/sulfate ratio, calculations of the direct radiative forcing of black carbon and sulfate aerosols as well as the forcing of an external mixture of both aerosols, based on global three-dimensional mass distributions of both aerosol components. Global monthly mean mass distributions of black carbon and sulfate were obtained from *Cooke and Wilson* [1996] and *Langner and Rodhe* [1991], respectively, for both January and July. These spatial and temporal distributions of aerosol mass are used in conjunction with estimated aerosol radiative properties to perform calculations for clear-sky conditions with a δ-Eddington method.

Models Used and Experiments

The model structure adopted in the present study is illustrated in Figure 1. The input data for the δ-Eddington radiation transfer model DELED were obtained as follows:

Global aerosol mass fields were generated with the transport model MOGUNTIA [*Zimmermann*, 1987; *Zimmermann et al.*, 1989; *Feichter and Crutzen*, 1990]; aerosol optical parameters were calculated from Mie theory, for estimated aerosol size distributions and refractive indices; and meteorological data and other ancillary global data fields were obtained from a

Paper number 97JD01863
0148-0227/97/97JD-01863$09.00

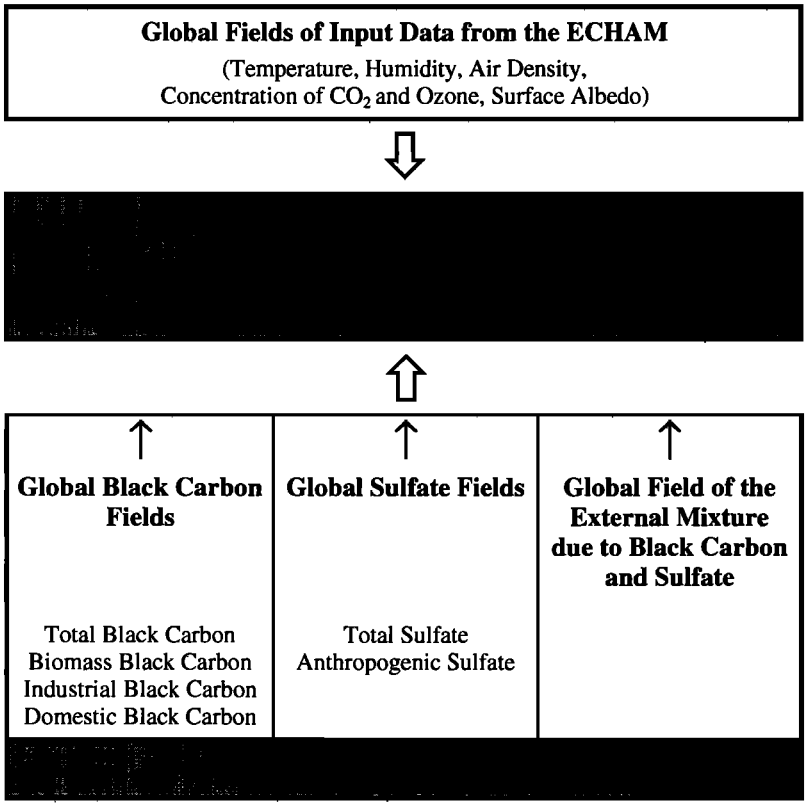

Figure 1. Model structure and input parameters for different experiments to calculate the radiative forcing by aerosols.

climatological run of the ECHAM GCM. The individual models used and the experimental design are explained in more detail in the following.

Aerosol Distribution

The basis for calculations of the radiative forcing are three-dimensional model simulations of the tropospheric black carbon and sulfur cycles. The global transport-chemistry model MOGUNTIA used to calculate the mass concentrations of both aerosol components has a horizontal resolution of 10° × 10° and 10 vertical layers from the surface up to 100 hPa. Advection takes place by climatological monthlymean winds. Transport processes occurring on smaller space and timescales are parameterized as eddy diffusion, except subgrid scale vertical exchange in convective clouds which is treated separately [*Zimmermann*, 1987; *Zimmermann et al.*, 1989; *Feichter and Crutzen*, 1990].

The model is used to calculate the monthly mean black carbon mass concentration as described in more detail by *Cooke and Wilson* [1996]. Their black carbon model uses fossil fuel consumption from a United Nations fuel use data set along with a compilation of biomass burning sources of black carbon. The annual emissions from fossil fuel combustion of 7.97 Tg and from biomass burning of 5.49 Tg are considered to be wholly anthropogenic. The model assumes black carbon to be hydrophobic and therefore not removed by wet precipitation when emitted, which ages to hydrophilic aerosol at an arbitrary rate [*Ogren*, 1982; *Crutzen et al.*, 1984; *Goldberg*, 1985]. The aged black carbon aerosol is assumed to have the same wet deposition characteristics as sulfate aerosol. The resulting turnover time is about a week with a global annual mean burden of black carbon of 0.27 Tg. *Cooke and Wilson* [1996] compare their calculations with observations of the surface concentration and find good agreement over the United States and Europe but with the tendency for their model to overpredict concentrations at remote sites. Their model results are comparable to another study from *Penner et al.* [1993].

Various experiments were performed to establish the contribution of industrial and domestic fossil fuel emissions and of biomass burning emissions of black carbon. Different size distributions could then be assumed for each of these sources in calculating the optical properties of the aerosol. As no measurements are available with global coverage, we used the same optical properties for all black carbon components.

The three-dimensional monthly mean sulfate distribution used here were calculated by *Langner and Rodhe* [1991]. Their scheme carries three species prognostically, dimethyl sulfide (DMS), sulfur dioxide (SO_2), and sulfate (SO_4). All biogenic emissions occur as DMS. SO_2 emissions from fossil fuel combustion, biomass burning, and from volcanoes are considered. The total sulfur emission amounts to 98 Tg per year, with 70 Tg from fossil fuel use and 2.5 Tg from biomass burning. The model treats the gaseous phase reactions of DMS and SO_2 with OH radicals. In the aqueous phase, all SO_2 is assumed to be oxidized to sulfate on entering a cloud (fast oxidation case). The resulting annual mean sulfate burden is 2.3 Tg and the turnover time of sulfate is 4.6 days. *Langner and Rodhe* [1991] performed two experiments, one with natural emissions only and one with natural and anthropogenic sources. The difference between these simulations, assumed to be due to anthropogenic emissions, were used for our forcing calculations.

The annual mean ratio between the black carbon and the sulfate mass integrated over the model domain is 0.12. Figure 2 presents the horizontal distribution of the ratio between black carbon and sulfate surface mixing ratios for January and July. Sulfate mixing ratios dominate black carbon mixing ratios except over regions

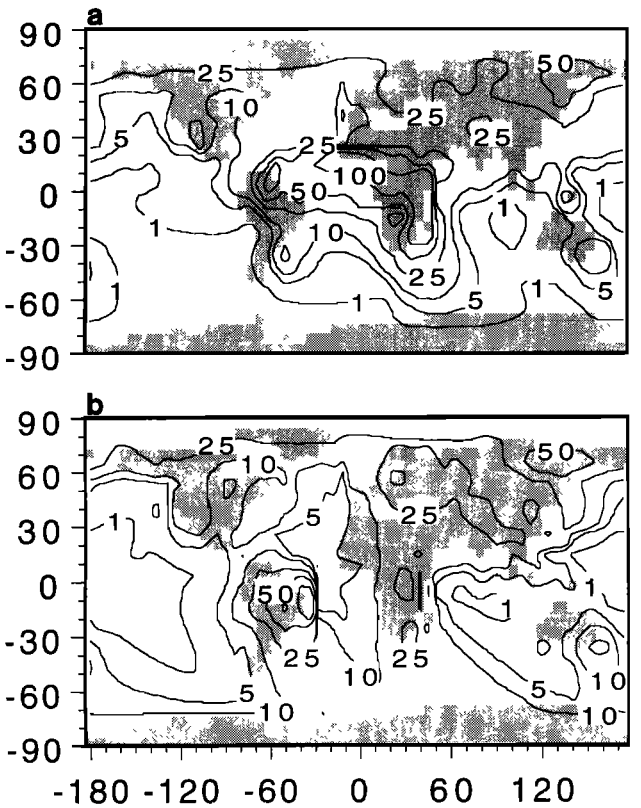

Figure 2. Calculated black carbon/ sulfate ratio at the surface in percent for (a) January and (b) July.

where biomass burning is important. A high ratio is also found in January over northeast Siberia and the Bering Sea due to quite low sulfate values. Over the eastern United States and western Europe the ratio is about 0.1. The black carbon to sulfate ratio is higher (" 0.20 - 0.50) over the southwestern United States, where sulfur emissions are low, and over Eastern Europe due to domestic coal burning. *Malm et al.* [1994] report, based on measurements, higher carbon/ammonium-sulfate ratios over the southwest United States than over the eastern United States (e.g., 0.36 over southern California and 0.11 over the northeastern United States). Whereas the black carbon mixing ratios do not show a distinct seasonal variation, the sulfate concentrations over the United States are higher in summer than in winter. This is in contrast to Europe where winter sulfate concentrations are higher, and consequently, the black carbon/sulfate ratios over Europe are higher by a factor of 2 in July than in January. *Haywood and Shine* [1995], who derived an atmospheric soot distribution based on sulfate concentrations to estimate the forcing of both aerosol types, assumed a constant ratio of 0.075 for fossil fuel use emissions only. The simulated ratios of the contribution from fossil fuel use are the same over Europe and the United States as the ratios shown above. Therefore we think that Haywood and Shine underestimate the atmospheric soot load by about a factor of 2. Moreover, they fail to account for the distinctly marked seasonal and geographical variability of the soot/sulfate ratio.

Radiation Model and Optical Properties of Aerosols

The radiative forcing calculations have been carried out with the one-dimensional radiation model [*Bakan*, 1982; *Bakan and Hinzpeter*, 1988; *Schult*, 1991] which has recently been used in a number of radiation estimates by aerosols within the climate model ECHAM by the name of DELED [*Bakan et al.*, 1991; *Graf et al.*, 1993; *Schult and Köpke*, 1994, 1995]. DELED solves the radiation transfer equation of the Earth atmosphere by using the δ-Eddington approximation [*Joseph et al.*, 1976] under the assumption of a plane parallel atmosphere. The radiation spectra are represented by eight wavelength intervals for the solar part (0.3 - 3.6 μm) and by 18 intervals for the terrestrial range (3.6 - 100 μm). However, the changes in the thermal infrared radiation by the aerosols considered were found to be small when compared to the effect on solar radiation and are therefore not further evaluated in this work.

The present version of DELED includes all important processes influencing the radiation transport: Rayleigh scattering, absorption by water vapor, carbon dioxide and ozone, as well as extinction by water droplets and aerosol particles at variable vertical resolution. The transmission function through the main absorber in each wavelength interval is approximated by a sum of exponentials series with the absorber amount and the absorption coefficients.

The main radiative forcing results have been calculated for a cloud free atmosphere, with calculations for a cloudy atmosphere providing a preliminary assessment of the effect of clouds on these forcings. The indirect radiative effects of aerosols on clouds, of changing the numbers of cloud droplets, and their optical properties were not investigated in this work.

Because the radiation model is developed especially for the investigation of different aerosols in the troposphere and stratosphere, optical parameters of different aerosol components of natural and anthropogenic sources are included in this model. In order to make reliable estimates of the effect of particles on the radiation budget, it is necessary to have data of the optical properties of particles for the full spectrum of wavelengths. On the basis of Mie theory the wavelength dependent optical parameters of sulfate and black carbon particles are determined from their

Table 1. Indices of Refraction of Aerosols Used Dependent of Wavelength λ According to *Köpke et al.* [1994]

λ	*Black Carbon*		*Sulfate, 0%*		*Sulfate, 80 %*	
μm	*n*	*k*	*n*	*k*	*n*	*k*
0.35	1.75	0.465	1.45	1.00×10^{-8}	1.37	7.22×10^{-9}
0.45	1.75	0.455	1.43	1.00×10^{-8}	1.36	2.85×10^{-9}
0.55	1.75	0.440	1.43	1.00×10^{-8}	1.35	3.60×10^{-9}
0.65	1.75	0.435	1.43	1.47×10^{-8}	1.35	1.61×10^{-8}
0.75	1.75	0.430	1.43	1.89×10^{-8}	1.35	1.28×10^{-7}
1.00	1.76	0.440	1.42	1.50×10^{-6}	1.35	2.61×10^{-6}
1.50	1.79	0.460	1.40	1.34×10^{-4}	1.34	1.16×10^{-4}
2.00	1.81	0.490	1.38	1.26×10^{-3}	1.32	1.13×10^{-3}
2.50	1.82	0.510	1.34	3.76×10^{-3}	1.28	2.41×10^{-3}
3.00	1.84	0.540	1.29	9.55×10^{-2}	1.36	2.36×10^{-1}
3.20	1.86	0.540	1.31	1.35×10^{-1}	1.44	1.01×10^{-1}
3.50	1.88	0.560	1.38	1.58×10^{-1}	1.39	3.98×10^{-2}
4.00	1.92	0.580	1.40	1.36×10^{-1}	1.36	3.14×10^{-2}
5.00	1.97	0.600	1.36	1.21×10^{-1}	1.33	3.46×10^{-2}
6.00	2.02	0.620	1.42	1.95×10^{-1}	1.30	4.84×10^{-2}
6.50	2.04	0.630	1.37	1.28×10^{-1}	1.35	5.73×10^{-2}
7.90	2.12	0.670	1.14	4.88×10^{-1}	1.26	1.27×10^{-1}
8.50	2.15	0.690	1.37	7.55×10^{-1}	1.30	1.83×10^{-1}
9.00	2.17	0.700	1.65	6.33×10^{-1}	1.34	1.61×10^{-1}
10.00	2.21	0.720	1.89	4.55×10^{-1}	1.36	1.33×10^{-1}

The *n* is the real part, *k* the imaginary part of the refractive index. Values of sulfate are given for 0% and 80 % relative humidity.

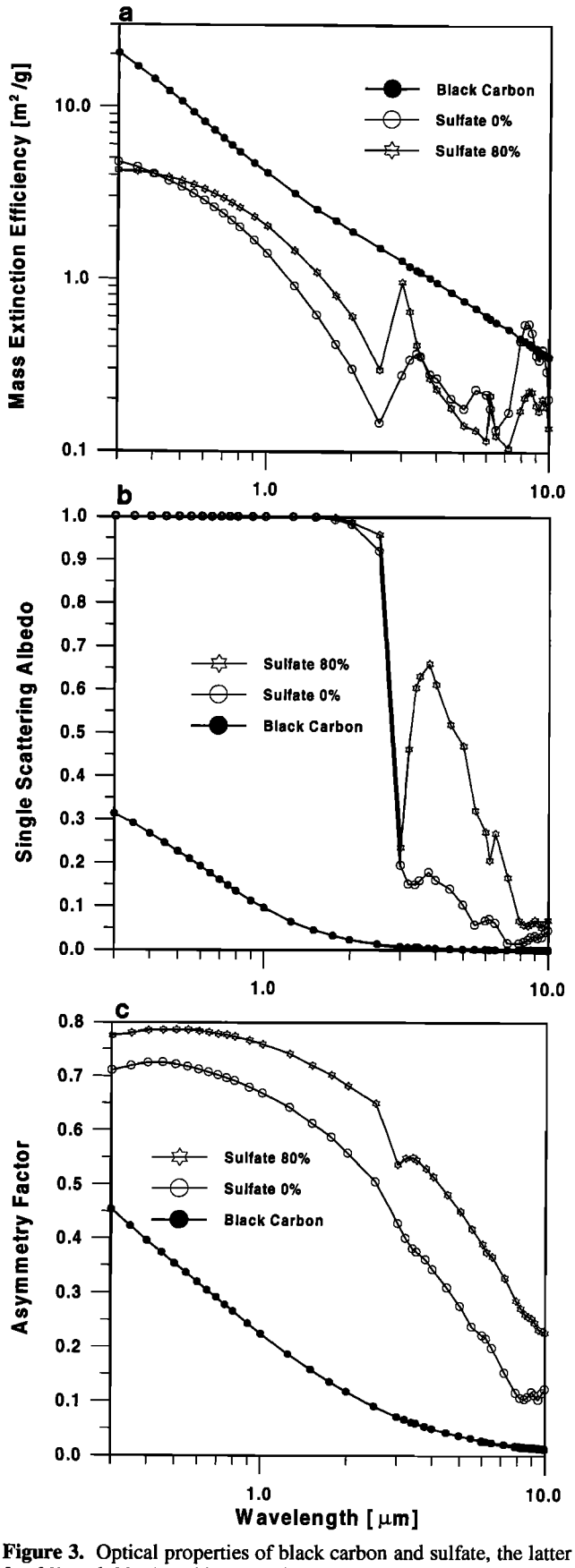

Figure 3. Optical properties of black carbon and sulfate, the latter for 0% and 80 % ambient relative humidity, resulting from Mie calculations; (a) mass extinction efficiency (m^2/g), (b) single-scattering albedo, and (c) asymmetry factor dependent on the wavelength.

complex refractive indices and characteristic particle size distributions. For these calculations we use the refractive indices from the global aerosol data set (GADS) [*Köpke et al.*, 1994] as presented in Table 1. The resulting optical parameters used, mass extinction efficiency, single-scattering albedo and asymmetry factor, are plotted in Figure 3 for black carbon and sulfate and show an extreme sensitivity against the wave-length.

The input parameters of soot for Mie calculations are also taken from *Shettle and Fenn* [1979] and fit nicely within the range found in the literature. As a consequence of the concept of external mixture of components, no internal mixture of soot with hygroscopic particles is assumed. Thus the size of the soot particles is not varied with relative humidity [*Dlugi*, 1989; *Ogren*, 1982; *Crutzen et al.*, 1984; *Goldberg*, 1985]. Although aged soot particles are fractal clusters, i.e., agglomerations of small, approximately spherical elements strung out in long, often multiconnected chains [*Bruce et al.*, 1991], the spheres in the agglomerate with a high density of 2.3 g/cm^3 act essentially as independent absorbers [*Colbeck et al.*, 1989]. The extinction calculations for black carbon are based on a size distribution of these small particles appropriate for the primary particles which form the "observed" black carbon agglomerates [*Twitty and Weinman*, 1971; *Patterson et al.*, 1991; *WMO*, 1983]. Because of the structure of this soot agglomerates with empty space between the elements we assume a relatively low particle density of 1 g/cm^3 for the mass efficiencies [*Horvath*, 1993].

The specific extinction coefficient at a wavelength of 0.5 μm is 10.6 m^2/g for black carbon particles with a lognormal size distribution with a mode radius of 0.012 μm and a sigma of 2.0. Experimentally determined values of mass extinction efficiency show the continuous decrease with wavelength [*Bruce et al.*, 1991]. The agreement of single-scattering albedo and mass absorption efficiency from Figure 3 with measured values is good [*Bruce et al.*, 1991; *Colbeck et al.*, 1989] (also a survey is given by *Liousse et al.* [1993]). It must be mentioned however that the data in the literature show a variability in the order of 2 due to the different methods and analyzed material.

Because of the lack of information or measurements of the size of particles on the global scale we have assumed that the size distributions are independent of humidity and spatially and temporally variable microphysical processes like wet and dry removal. We also assume that the optical parameters of black carbon particles remain independent of humidity, while the calculations of the sulfate optical parameters are for a constant relative humidity of 80%, implying an internal mixture of sulfate and water. For sulfate the growth of particles with increasing relative humidity has been considered, as specified by *d'Almeida et al.* [1991].

For sulfate particles the specific extinction coefficient is 3.7 m^2/g with a mode radius of 0.118 μm and a sigma of 2.03 and a density of 1.14 g/cm^3 [*Köpke et al.*, 1994] for ambient conditions of 80% relative humidity. The assumed density for sulfate is equivalent to sulfuric acid solution droplets with water, but we did the computations additionally with a particle density of 1.0 g/cm^3 as a lower limit. Note that the extinction coefficients of ammonium sulfate are approximately equal to sulfuric acid solution assumed. Only in the spectral interval between 1 and 2.5 μm the extinction coefficients are greatly different due to higher absorption efficiency [*Toon et al.*, 1976]. The resulting single-scattering albedos are 0.23 for black carbon at 0.5 μm and 1.0 for sulfate.

The aerosol mass fields were interpolated to the T21 resolution of the global circulation model ECHAM (5.6° horizontal resolution, 19 vertical layers up to stratosphere) [*Roeckner et al.*, 1992]. Monthly means of the three-dimensional meteorological fields required as input parameters for DELED were taken from a

30 year climatological run of ECHAM. Surface albedo, ozone, and carbon dioxide concentration fields were used from ECHAM.

Radiative forcings were then calculated by using the DELED code to calculate the net solar fluxes at the top of the troposphere (150 hPa) with and without the aerosol fields, for each column of the T21 grid, and for January and July. The difference between the net solar fluxes is the aerosol forcing. Results represent mean values averaged over daylight hours.

Sensitivity Studies

The purpose of these preliminary experiments was to demonstrate the dependence of radiative forcing on parameters like the solar zenith angle and the surface albedo in order to understand better the resulting global forcing patterns that result from the following calculations.

Three different calculations with the one-dimensional radiation model were carried out using different aerosols and climatologically representative northern hemisphere summertime conditions. These calculations were performed for typical optical depths over Europe at 0.5 μm of 0.01 and of 0.03 for black carbon and sulfate, respectively, and an optical depth of the external mixture of both components of 0.04. A surface albedo of 0.16 characteristic of northern hemisphere midlatitude continents was assumed. For the calculation of the radiative forcing by aerosols the experiment was repeated without aerosol particles.

Figure 4 shows the resulting anomalies in the top solar forcing as a function of the zenith angle of the Sun. It is interesting to note that the black carbon forcing is always positive and increases nearly linearly with decreasing zenith angle, while the sulfate forcing is always negative but with a much smaller slope and a minimum at zenith angles typical of midlatitude wintertime. The behavior of the externally mixed aerosol differs from the sum of the effects of the individual components; due to interactions of the absorbing black carbon particles with the scattering processes of sulfate particles, the positive forcing of black carbon increasingly dominates the forcing of the mixture if the zenith angle decreases.

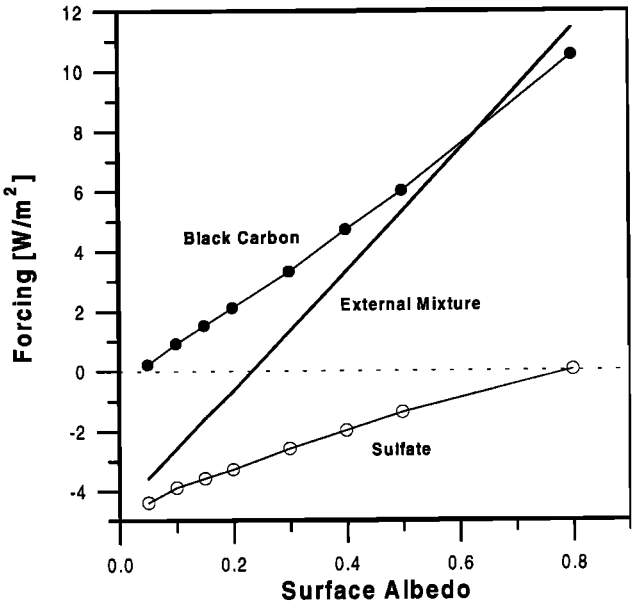

Figure 5. Top solar forcing of typical concentrations of black carbon and of sulfate aerosols as well as of their external mixture depending on the surface albedo. The Sun zenith angle is 60°.

The influence of the underlying surface on the forcing at a fixed zenith angle of 60° is illustrated in Figure 5. All three aerosol types show a positive, nearly linear increase in the forcing with increasing surface albedo. Similarly to the effect of varying the zenith angle, the positive forcing effect of the black carbon aerosol increasingly dominates the forcing effect of the external mixture if the surface albedo increases. An interesting feature is that the external mixture shows a positive forcing at higher surface albedo such as over white sands or snowcovered surfaces.

Further sensitivity calculations were carried out for sulfate under different relative humidity conditions. We assume that the particle number density of sulfate is equal in all cases but the

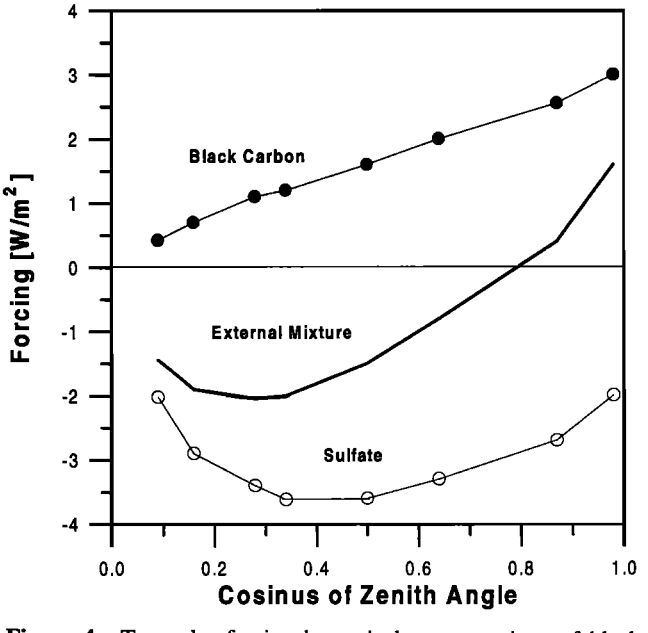

Figure 4. Top solar forcing by typical concentrations of black carbon, sulfate, and their external mixture as function of the cosine of Sun zenith angle. The surface albedo is assumed 0.16.

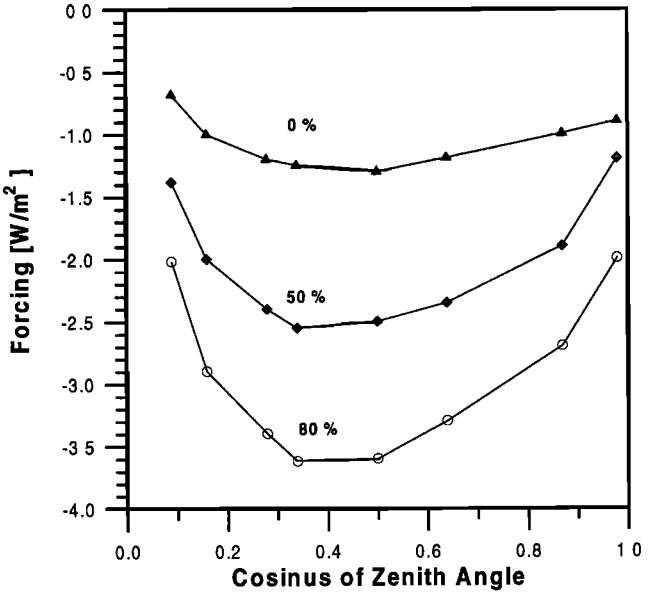

Figure 6. Top solar forcing of sulfate aerosol for different ambient relative humidities as function of the cosine of Sun zenith angle. The surface albedo is assumed 0.16.

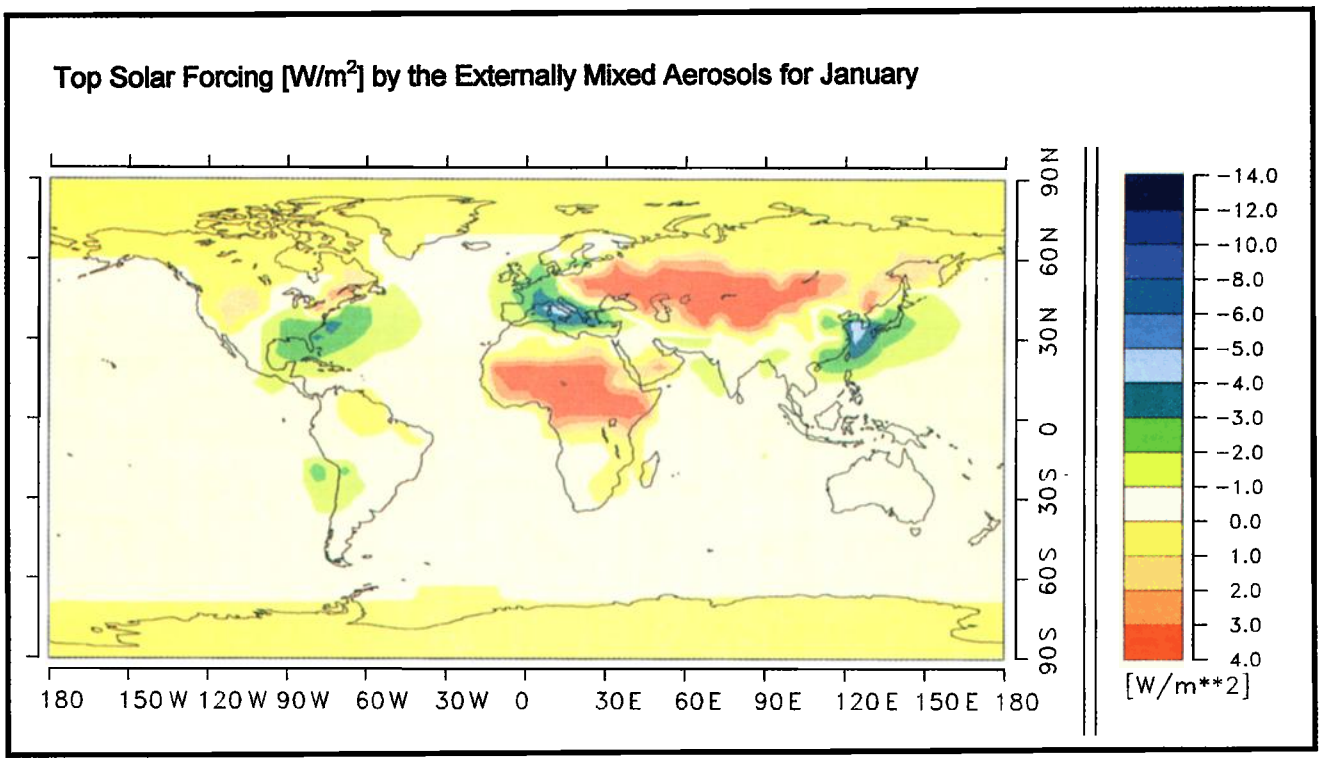

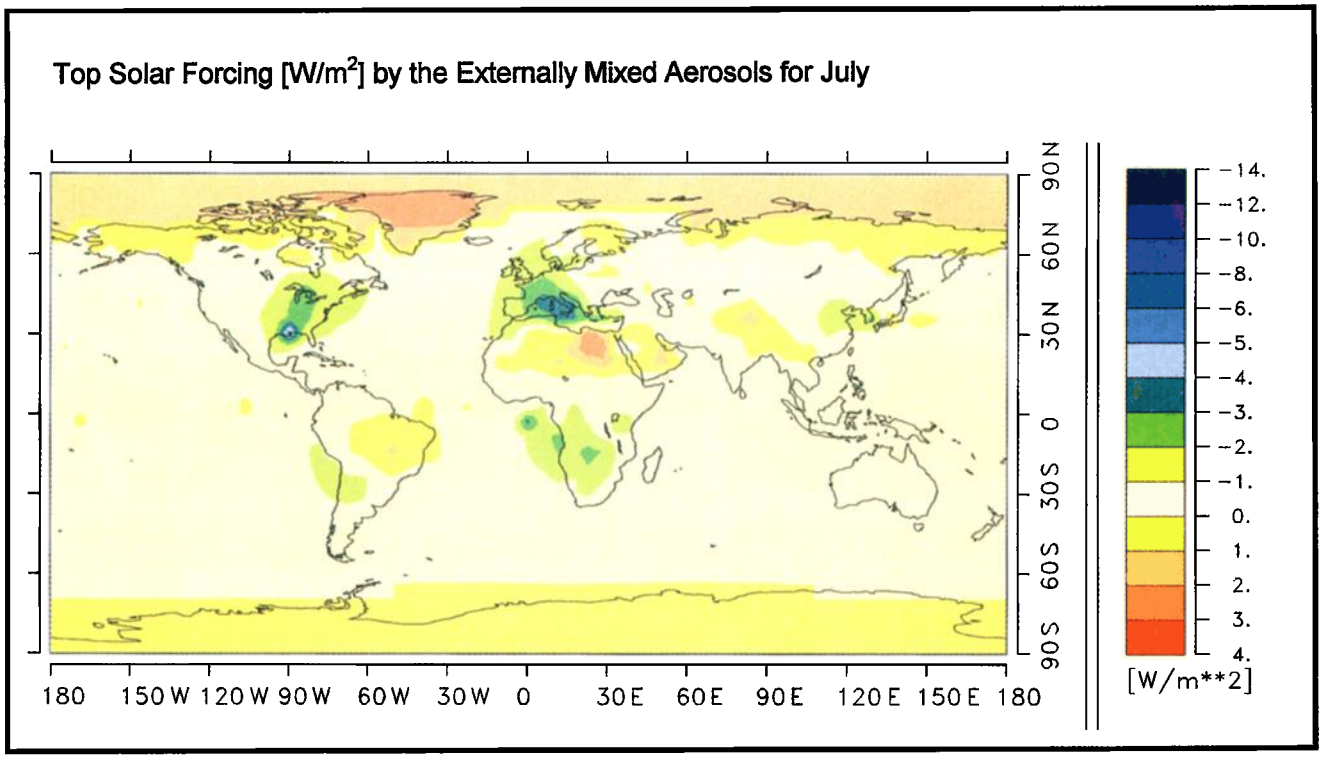

Plate 1. Top solar radiative forcing of externally mixed aerosols consisting of black carbon and sulfate for (a) January and for (b) July.

particles grow with increasing humidity. These results, presented in Figure 6 for varying zenith angles, show the strong influence of the humidity. In summary, our estimates of the forcing with fixed relative humidity of 80 % may be regarded as a simplification but may be justified regarding the uncertainties of the size distribution and of the aerosol mixture.

Results

In this section we present the calculated optical depths based on the results of the transport model MOGUNTIA in conjunction with the assumed optical parameters. The resulting global radiative forcing fields due to black carbon, sulfate, and an external mixture of both are discussed. For the interpretation and comparison of the results we use zonal mean values, although it should be noted that the global patterns are highly variable.

Radiative Forcing due to Black Carbon Aerosols

Figure 7 shows the zonally averaged optical depth at a wavelength of 0.5 μm for the total black carbon load within the atmosphere and the contributions thereof from biomass burning, domestic and industrial sources for January. As expected, the optical depth is high over the main anthropogenic source regions of the northern hemisphere midlatitudes. The peak zonal mean optical depth occurs over the tropical latitudes, and it is dominated by the contribution from biomass burning in the African savannas which alone gives a zonal mean optical depth of 0.005. The optical depths for July are significantly smaller, with a global mean of 0.0017 compared to 0.0026 in January, and are therefore not shown here.

Zonal mean forcings, defined as the anomaly of the net solar radiation at top of the troposphere, due to black carbon particles and the contributions of the carbon sources, are shown in Figure 8 for January. Figure 9 shows the radiative forcings due to the total black carbon field for January and July. Global and northern hemispherical means of the forcing of the different black carbon scenarios are listed in Table 2.

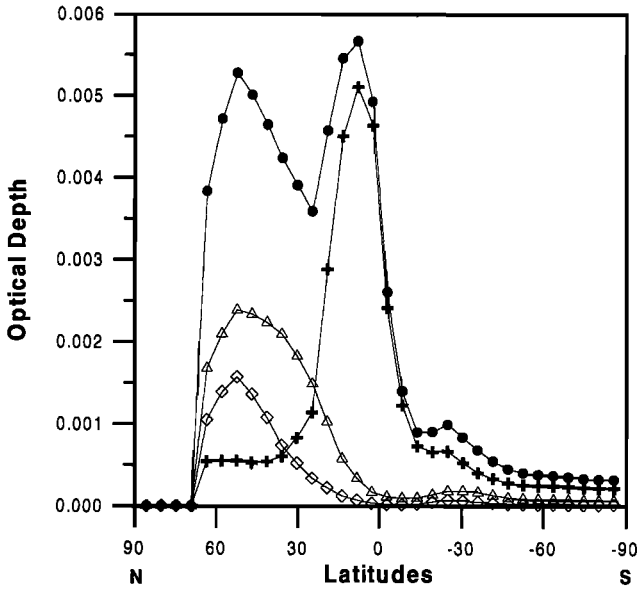

Figure 7. Zonal means of optical depth of black carbon from different sources based on MOGUNTIA calculations for January (circles, total black carbon; pluses, biomass burning; triangles, industrial black carbon; diamonds, domestic black carbon).

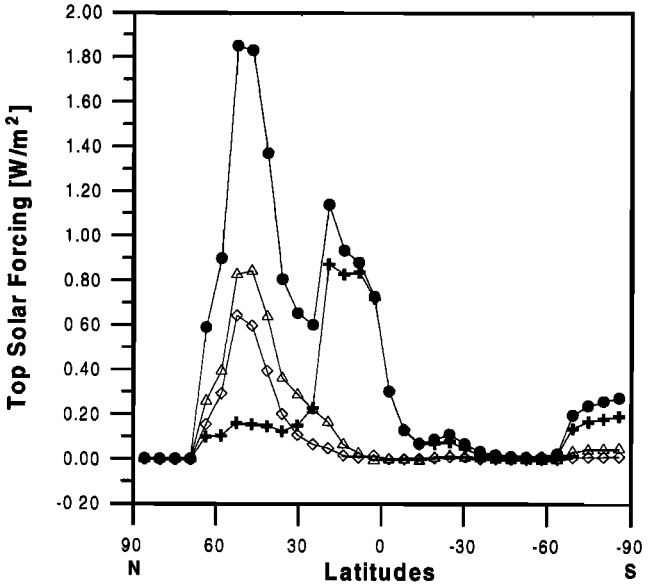

Figure 8. Zonal means of top solar radiative forcing by black carbon of different sources based on MOGUNTIA calculations for July (circles, total black carbon; pluses, biomass burning; triangles, industrial black carbon; diamonds, domestic black carbon).

The zonal mean forcing is positive at all latitudes in both months, which means that black carbon aerosols decrease the planetary albedo of the Earth's atmosphere. The reason for this not obvious result is that the scattering is low because we assume such a small particle size for black carbon particles (Mie calculations give an increasing single-scattering albedo for an increasing mode radius; for instance, the single-scattering albedo at a wavelength of 0.5 μm is 0.42 for a mode radius of 0.05 μm). The peak forcing in January of 1.8 W/m^2 occurs in high northern latitudes where the surface albedo is high due to snowcover. Although the maximum optical depth occurs over the savanna regions of Africa, the maximum forcing of ~1 W/m^2 is found farther north over the Sahara where the surface albedo is relatively higher. In July the

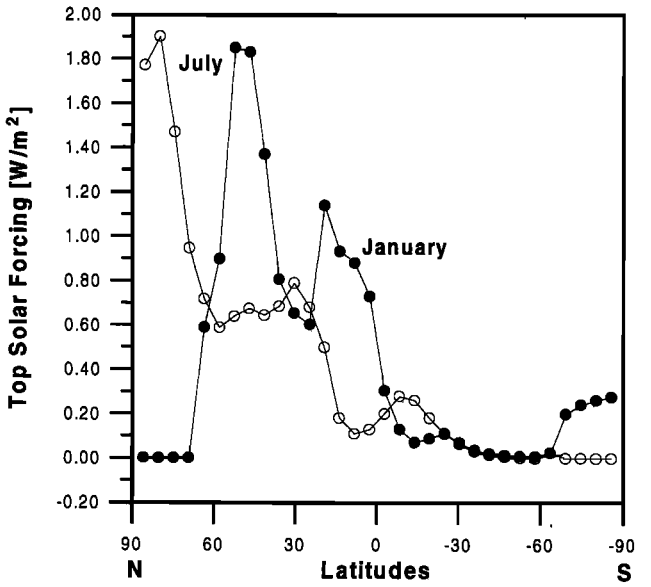

Figure 9. Zonal means of top solar radiative forcing by total black carbon based on MOGUNTIA calculations for January and July.

Table 2. Mean Values of Radiative Forcing by Different Black Carbon Aerosols at the Top of the Atmosphere [W/m^2] Based on MOGUNTIA Calculations for January and July (in parentheses) Under Cloudless Conditions

	January (July)			
		Northern Hemisphere		
Experiment	Mean	Mean	Land	Ocean
Total black carbon aerosols	0.51 (0.34)	0.92 (0.57)	2.03 (0.96)	0.18 (0.32)
Black carbon of biomass burning	0.24 (0.06)	0.39 (0.04)	0.86 (0.09)	0.08 (0.01)
Industrial and traffic black carbon	0.14 (0.15)	0.28 (0.30)	0.61 (0.48)	0.06 (0.18)
Domestic black carbon	0.09 (0.06)	0.17 (0.12)	0.39 (0.22)	0.02 (0.06)

maximum forcing is found over the polar region of the northern hemisphere which is covered by ice; however, the forcing over the northern hemisphere middle and tropical latitudes is lower, due to the smaller optical depths. Local maxima are about 4 W/m^2 over the Sahara in July and 7 W/m^2 over the Sahara and Eastern Europe in January, respectively. The global mean forcing is higher in January with 0.51 W/m^2 than in July with 0.34 W/m^2 mainly due to the higher surface albedo in the northern hemisphere winter and the seasonal variation of the sources. As indicated in Table 2, most of the differences in the forcing between January and July occurs over northern hemisphere continents. It should also be noted that mainly due to the low surface albedo the effect of black carbon on the short wave radiation budget over the ocean is negligible.

Forcing by Natural and Anthropogenic Sulfate

Unlike black carbon, the global sulfate fields include a natural component. We have therefore determined the anthropogenic sulfate forcing by carrying out two experiments and subtracting the resulting natural from the total sulfate top solar anomalies.

In contrast to the effect of black carbon particles, the reflected irradiance at the top of the atmosphere is increased by sulfate aerosols. Figure 10 shows the zonally averaged anomalies of the net solar radiation by sulfate at the top of the troposphere for January. The strongest forcing, of the order of -2 W/m^2, occurs in the northern hemisphere midlatitudes where anthropogenic sulfur emissions are highest. Over the southern hemisphere the zonally averaged forcing due to anthropogenic sulfate is in the range of 0 to -0.5 W/m^2. In that region, the influence of the natural sulfate aerosol produced by marine activity and volcanoes prevail.

Local peak values of about -5 W/m^2 were found over Europe and Southeast Asia in January. Both the geographical distribution and the magnitude of the sulfate forcing agree quite well with that estimated by *Charlson et al.* [1991]. The resulting global mean forcing due to anthropogenic sulfate aerosols is -0.69 W/m^2 in January and -0.63 W/m^2 in July compared to -0.60 W/m^2 as given by *Charlson et al.* [1991]. Our values are, however, for clear-sky conditions, whereas *Charlson et al.* [1991] corrected their value for an assumed global mean cloudcover of 61%. Similarly, correcting for the clear-sky fraction would lower our estimate substantially, particularly in January when the cloudcover over Europe and eastern United States is high. We would then expect a global annual mean forcing closer to the estimates of *Kiehl and Briegleb* [1993] who report a value of -0.28 W/m^2.

Radiative Forcing by an External Mixture of Black Carbon and Anthropogenic Sulfate

Finally, the radiative forcing of a mixture of anthropogenic sulfate and black carbon aerosol is investigated. Because anthropogenic sulfate and black carbon emissions have common sources, anthropogenic aerosol contains a mixture of both. Therefore a realistic estimate of the sign and magnitude of the anthropogenic aerosol forcing should consider both aerosol types together, since the sensitivity studies have shown that the combined radiative effects are not the sum of the individual effects. However, because of the lack of information on the state of mixing of anthropogenic sulfate and black carbon aerosol, which determines its optical properties, we have assumed an external mixture.

The external mixture has an optical depth corresponding to the sum of the individual black carbon and sulfate fields. The extinction and absorption coefficients are calculated by weighting the parameters of the contributing components by their respective mixing ratios. Other optical parameters needed for our calculation such as the asymmetry factor are taken as the product of the asymmetry factor and the weighted scattering coefficient of the single components normalized to the total scattering coefficient of the mixture.

The forcing caused by the externally mixed aerosol is not equal to the sum of the forcing of the individual aerosol components due to the nonlinear interaction of the scattering and absorption processes. Considering the top solar radiative forcing shown in Plate 1a for January, it appears that the sign of the forcing by the external mixture is sensitive to the mixing ratio between sulfate and black carbon and to the surface albedo. For example, the negative forcing over the industrial regions of western Europe, North America and the east coast of Asia is associated with high-sulfate mass. Areas of positive forcing over central Asia and Africa, on the other hand, are found where black carbon mass loadings are high and where the surfaces are highly reflective, such

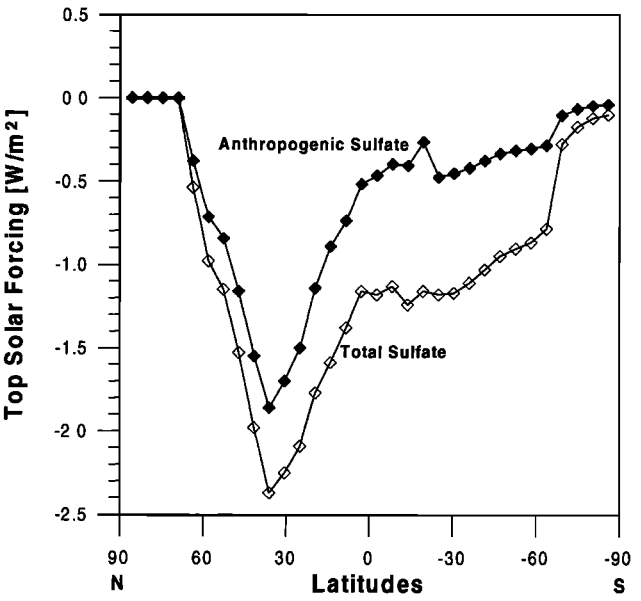

Figure 10. Zonally averaged values of top solar radiative forcing of total and anthropogenic sulfate based on MOGUNTIA calculations for January.

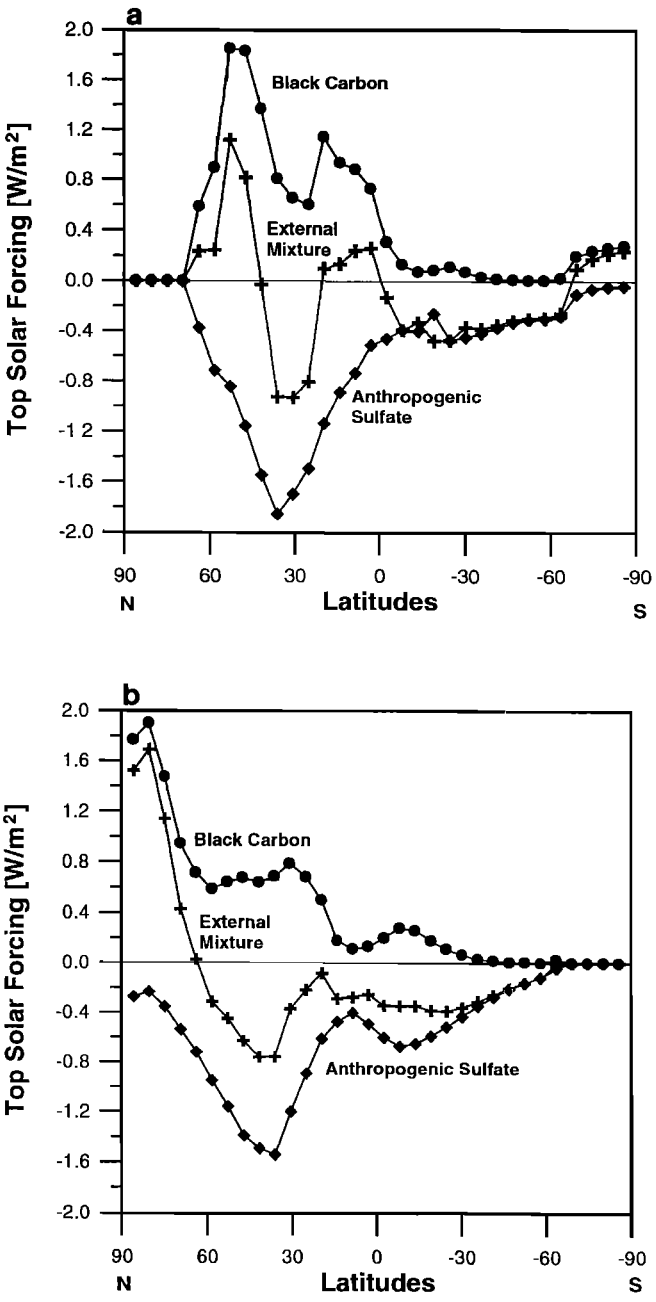

Figure 11. Zonally averaged values of top solar radiative forcing of black carbon, sulfate, and their external mixture for (a) January and for (b) July.

as snow, ice, or desert. In July the black carbon and sulfate mass loadings are lower and the surface over northern Europe and Asia less reflective, therefore the forcing is much smaller and the high positive values over Eurasia disappear, as shown in Plate 1b.

The zonal mean radiative forcing due to the external mixture of black carbon and sulfate is compared with the zonal mean forcings for the individual components in Figures 11a and 11b for January and July, respectively. Although the global mean radiative forcing of the external mixture is as expected negative, because of the reduction of solar radiation due to scattering, locally positive forcing can be observed due to the high-absorption efficiency of black carbon, particularly during the northern hemisphere winter.

Discussion and Conclusion

We calculated the radiative forcing by anthropogenic aerosols as mixture of sulfate and black carbon. The estimate is based on the three-dimensional monthly mean aerosol mass distribution simulated by a global tracer transport model. In addition to the mass distribution of atmospheric aerosols it is necessary to know the radiative properties of the aerosols. In the absence of detailed measurements of these aerosol parameters we have assumed characteristic size distributions and chemical composition for Mie calculations of the relevant optical properties of black carbon and sulfate aerosol for the 26 wavelength ranges used in the radiative transfer model. The final results for the different experiments are summarized in Table 3 as global and northern hemispheric averages.

In the black carbon experiment, the solar radiative forcing at the top of the troposphere is positive and ranges between a global mean of 0.5 W/m^2 in January and 0.3 W/m^2 in July. The forcing occurs predominantly in the northern hemisphere; in both months the mean over the southern hemisphere is only 0.1 W/m^2. These calculated forcings are, however, subject to considerable uncertainty, due to the neglect of humidity dependencies of black carbon extinction and an explicit treatment of aerosol physics. A differentiation of the optical properties and size distribution of black carbon aerosol depending on the source is really needed to reduce the uncertainties. Since the black carbon aerosol from biomass burning contributes most to the radiative forcing, the investigation of the size distribution of biomass burning aerosol products, their chemical composition, and optical properties has perhaps the greatest priority.

The calculated forcing by the anthropogenic sulfate aerosol is negative, as has been estimated previously, with a global mean of -0.7 W/m^2 for a cloud free global atmosphere, assuming that the

Table 3. Globally and Northern Hemispherical Averaged Values of Solar Forcing by Black Carbon, Sulfate Aerosols, and Externally Mixed Aerosols at the Top of Troposphere [W/m^2] Based on MOGUNTIA Calculations for January and July Under Cloudless Conditions.

	January		July	
	Global Mean	Northern Hemi-spherical Mean	Global Mean	Northern Hemi-spherical Mean
Total black carbon aerosols	0.51	0.92	0.34	0.57
Total sulfate aerosols	-1.26	-1.50	-1.23	-1.63
Anthropogenic sulfate aerosols	-0.69	-1.02	-0.63	-0.87
Anthropogenic sulfate aerosols with density = 1.0 g/cm^3	-1.14	-1.64	-1.03	-1.42
External mixture of anthropogenic sulfate and black carbon	-0.16	-0.01	-0.26	-0.25
External mixture of anthropogenic sulfate (density = 1.0 g/cm^3) and black carbon	-0.56	-0.61	-0.64	-0.77

aerosol is H_2SO_4 solution at 80 % relative humidity. Assuming a density of 1 g/cm^3 gives an upper limit forcing of -1.1 W/m^2, which clearly indicates the sensitivity of the aerosol optical properties to the size distribution and composition of the aerosol, and which play a significant role in the calculated radiative fluxes. Again, we have assumed a single global size distribution and composition for the sulfate aerosol, whereas in reality there is considerable local variation.

These aspects have to be solved with an interactively coupled aerosol-climate model including the sources and sinks of particles. In addition, it is important to consider particles of different sizes because the radiative effect depends mainly on the particle size. However, investigations of the influence of different aerosols on global climate are at an initial stage.

A complete estimate of climate changes due to man-made activities needs to consider all atmospheric constituents of anthropogenic origin, not only the greenhouse gases but also the different aerosols, mainly consisting of sulfate and black carbon. Assuming a simple external mixture, we calculate a relatively small global mean top solar forcing of -0.1 to -0.3 W/m^2. According to *Haywood and Shine* [1995] the assumption of the internally mixed soot/sulfate aerosol leads to a less negative forcing (≈25%) compared to calculations with an external mixture. However, even with the simple assumption of an external mixture the combined effect of sulfate and black carbon is different to the sum of the individual effects, and we find an inhomogeneous spatial distribution of the forcing which can locally change the positive forcing due to the greenhouse gases. Black carbon particles can mask the negative forcing of predominantly scattering aerosols. During the northern hemisphere winter in particular, the black carbon content tends to reduce the negative forcing by sulfate and therefore leads to a net warming effect. Again, more specific investigations are necessary to better understand the extent of mixing of such anthropogenic aerosols and their optical properties.

We recalculated the forcing considering the effect under cloudy conditions based on the monthly averaged three-dimensional cloud cover distribution and liquid water distribution of ECHAM. The sulfate forcing is weakened due to the shielding effect of the clouds, whereas the black carbon forcing is slightly enhanced. A stronger enhancement under cloudy conditions is found in the radiative forcing of the external mixture due to an increase of absorption caused by multiple scattering. It should, however, be noted that all interactions between aerosols and cloud optical properties are neglected in this case. These interactions will be the subject of further studies.

In future climate change scenarios, changes of aerosol parameters, such as the absorption efficiency of particles, need to be taken into account. Our calculations show that the black carbon content of the aerosol can influence the sign of the forcing. Trend analysis by *Arends et al.* [1994] has identified a significant decrease in the sulfate mixing ratio over Europe, which would imply a reduction of the negative forcing by this aerosol component. It seems, however, that other compounds like nitrate or organics show an increase which will be as important for scattering processes as sulfate [*Ten Brink et al.*, 1995; *Liousse et al.*, 1995, 1996].

The large uncertainties associated with changes in the size distribution and the chemical composition of aerosols from preindustrial to present-day conditions and for future scenarios limits a realistic climate change prediction. Finally, these results illustrate the importance of more precise knowledge about the aerosol quantities in determining their influence on the global radiation budget and their impact on climate.

References

Arends, B. G., H. M. Ten Brink, A. Waijers-Ijpelaan, and J. H. Baar, Trend-analysis of sulfate aerosol in Europe, *ECN-Rep.*, 52 pp., EC-Proj., Petten, Netherlands, 1994.

Bakan, S., Strahlungsgetriebene Zellularkonvektion in Schichtwolken, 99 pp., Ph. D. thesis, Univ. Hamburg, Germany, 1982.

Bakan, S., and H. Hinzpeter, Atmospheric radiation, in *Landolt-Börnstein*, Neue Ser., vol. 4b, pp. 110-186, Springer-Verlag, New York, 1988.

Bakan, S., et al., Climate response to smoke from the burning oil wells in Kuwait, *Nature, 351*, 367-371, 1991.

Bruce, C. W., T. F. Stromberg, K. P. Gurton, and J. B. Mozer, Trans-spectral absorption and scattering of electromagnetic radiation by diesel soot, *Appl. Opt., 30*, 1537-1546, 1991.

Charlock, T. P., K. Kondratyev, and M. Prokofyev, Review of recent research on the climate effect of aerosols, in *Aerosol Effects on Climate*, edited by S. G. Jennings, pp. 233-274, Univ. of Ariz. Press, Tucson, 1993.

Charlson, R. J., and J. Heintzenberg (Eds.), *Aerosol Forcing and Climate*, 416 pp., John Wiley, New York, 1995.

Charlson, R. J., J. Langner, H. Rodhe, C. B. Leovy, and S. G. Warren, Perturbation of the Northern Hemisphere radiative balance by backscattering from anthropogenic sulfate aerosols, *Tellus, 43*(AB), 152-163, 1991.

Colbeck, I., E. J. Hardman, and R. M. Harrison, Optical and dynamical properties of fractal clusters of carbonaceous smoke, *J. Aerosol Sci., 30*, 765-774, 1989.

Cooke W. F., and J. J. N. Wilson, A global black carbon aerosol model, *J. Geophys. Res., 101*, 19,395-19,409, 1996.

Crutzen, P. J., I. Galbally, and C. Bruehl, Atmospheric effects from post nuclear fires, *Clim. Change, 6*, 323-364, 1984.

d'Almeida, G. A., P. Köpke, and E. P. Shettle, *Atmospheric Aerosols: Global Climatology and Radiative Characteristics*, 561 pp., A. Deepak, Hampton, Va., 1991.

Dlugi, R., Chemistry and deposition of soot particles in moist air and fog, *Aerosol Sci. Tech., 10*, 93-105, 1989.

Feichter, J., and P. J. Crutzen, Parameterization of deep cumulus convection in a global tracer transport model, and its evaluation with 222Rn, *Tellus, 42*(B), 100-117, 1990.

Goldberg, E. D., *Black Carbon in the Environment: Properties Distribution*, John Wiley, New York, 1985.

Graf, H. F., I. Kirchner, A. Robock, and I. Schult, Pinatubo eruption winter climate effects: Model versus observations, *Clim. Dyn., 9*, 81-93, 1993.

Grassl, H., What are the radiative and climatic consequences of a changing concentration of atmospheric aerosol particles? in *The Changing Atmosphere*, edited by F.S. Rowland and I.S.A. Isaksen, pp. 187-199, John Wiley, New York, 1988.

Haywood, J. M., and K. P. Shine, The effect of anthropogenic sulfate and soot aerosol on the clear sky planetary radiation budget, *Geophys. Res. Lett., 22*, 603-606, 1995.

Horvath, H., Atmospheric light absorption, A review, *Atmos. Environ., 27*(A), 293-317, 1993.

Intergovernmental Panel on Climate Change (IPCC), *Climate Change*, edited by J.T. Houghton, B.A. Callander, and S.K. Varney, Cambridge University Press, New york, 1992.

Joseph, K. J., W. J. Wiscombe, and J. A. Weinman, The delta-Eddington approximation for radiative transfer, *J. Atmos. Sci., 33*, 2452-2459, 1976.

Kiehl, J. T., and B. P. Briegleb, The relative role of sulfate aerosols and greenhouse gases in climate forcing, *Science, 260*, 311-314, 1993.

Köpke, P., M. Hess, I. Schult, and E. Shettle, Global aerosol data set (GADS), in *Abstracts on the Fourth International Aerosol Conference*, edited by R.C. Flagan, pp. 420-421, Los Angeles, Calif., August 29 - September 2, 1994.

Kondratyev, K. Y., V. A. Ivanov, D. V. Pozdnyakov, and M. A. Prokofyev, Natural and anthropogenic aerosols: A comparative analysis, in *Chemical Events in the Atmosphere and Their Impact on the Environment*, edited by G. B. Marini-Bettolo, 56 pp., Pontif. Acad. Sci. Scr. Varia, Vatican City, 1983.

Langner, J., and H. Rodhe, A global three-dimensional model of the tropospheric sulfur cycle, *J. Atmos. Chem.*, *13*, 225-263, 1991.

Liousse, C., H. Cachier, and S. G. Jennings, Optical and thermal measurements of black carbon aerosol content in different environments: Variation of the specific attenuation cross-section, sigma (σ), *Atmos. Environ.*, *27*(A), 1203-1211, 1993.

Liousse, C., C. Devaux, F. Dulac, and H. Cachier, Aging of Savanna biomass burning aerosols: Consequences on their optical properties, *J. Atmo. Chem.*, *22*, 1-17, 1995.

Liousse, C., J. E. Penner, C. Chuang, J. J. Walton, and H. Eddleman, A global three-dimensional model study of carbonaceous aerosols, *J. Geophys. Res.*, *101*, 19,411-19,432, 1996.

Malm W. C., J. F. Sisler, D. Huffmann, R. E. Eldred, and T. A. Cahill, Spatial and seasonal trends in particle concentration and optical extinction in the United States, *J. Geophys. Res.*, *99*, 1347-1370, 1994.

Ogren, J. A., Deposition of particulate elemental carbon from the atmosphere, in *Particulate Carbon: Atmospheric Life Cycle*, edited by G. T. Wolff and R. L. Klimisch, Plenum, New York, 1982.

Patterson, E. M., R. M. Duckworth, C. M. Wyman, E. A. Powell, and J. W. Gooch, Measurements of the optical properties of the smoke emissions from plastics, hydrocarbons, and other urban fuels for nuclear winter studies, *Atmos. Environ.*, *25*(A), 2539-2552, 1991.

Penner, J. E., R. Dickinson, and C. O'Neill, Effects of aerosol from biomass burning on the global radiation budget, *Science*, *256*, 1432-1434, 1992.

Penner, J.E., H. Eddleman, and T. Novakov, Towards the development of a global inventory for black carbon emissions, *Atm. Environ*, *27*(A), 8, 1277-1295, 1993.

Roeckner, E., et al., Simulation of the present day climate with the ECHAM-MODEL: Impact of model physics and resolution, *Max-Planck-Inst. Meteorol. Tech. Rep 93*, Max Planck Inst. for Meteorol., Hamburg, Germany, 1992.

Schult, I., Bildung und Transport von Aerosolteilchen in der Stratosphäre und ihre Bedeutung für den Strahlungshaushalt, 142 pp., Ph. D. thesis, Examensarb., Max-Planck-Inst. für Meteorol., Hamburg, Germany, 1991

Schult, I., and P. Köpke, Aerosol forcing based on global aerosol data set, in *Abstracts on the Fourth International Aerosol Conference*, edited by R.C. Flagan, pp. 668-669, Los Angeles, Calif., August 29 - September 2, 1994.

Schult, I., and P. Köpke, Global radiative forcing by aerosols based on the global aerosol data set, *Ann. Geophys.*, 13, C389, 1995.

Shettle, E. P., and R. W. Fenn, Models of the aerosols of the lower atmosphere and the effects of humidity variations on their optical properties, *AFGL Tech. Rep.*, *AFGL-TR-7 9-0214*, 94 pp., Air Force Geophys. Lab., Bedford, Mass., 1979.

Taylor, K. E., and J. E. Penner, Climate system response to aerosols and greenhouse gases: A model study, *Nature*, *369*, 734-737, 1994.

Ten Brink, H. M., H. Graßl, I. Schult, G. Maracchi, M. Bindi, J. A. Scott, R. Dlugi, and V. Russak, Reduction of the solar radiation by manmade aerosol in Europe, *Summary Rep. EC-Proj. EV5V-CT92-0171*, 54 pp., Petten, Netherlands, 1995.

Toon, O. B., J. B. Pollack, and B. N. Khare, The optical constants of several atmospheric aerosol species: Ammonium sulfate, aluminium oxide, and sodium chloride, *J. Geophys. Res.*, *81*, 5733-5748, 1976.

Twitty, J. T., and J. A. Weinman, Radiative properties of carbonaceous aerosols, *J. Appl. Meteorol.*, *10*, 725-731, 1971.

Weiss, R. E., and A. P. Waggoner, Optical measurements of airborne soot in urban, rual, remote locations, in *Particle Carbon: Atmospheric Life Cycle*, edited by G. T. Wolff, and R. L. Klimisch, 317-324, Plenum, New York, 1982.

World ;Meteorological Organization (WMO), *Report of the Experts Meeting on Aerosols and Their Climatic Effects*, edited by A. Deepak and H. E. Gerber, 107 pp., *WCP-55*, Geneva, 1983.

Zimmermann, P. H., MOGUNTIA: A handy global tracer model, in Proceedings of the Sixteenth NATO/CCMS International Technical Meeting on Air Pollution Modeling and Its Application, D. Reidel, Norwell, Mass., 1987.

Zimmermann, P. H., J. Feichter, H. K. Rath, P. J. Crutzen, and W. Weiss, A global three-dimensional source receptor model investigation using Kr85, *Atmos. Environ.*, *23*, 25-35, 1989.

J. Feichter and I. Schult, Max-Planck-Institut für Meteorologie, Bundesstr 55, 20146 Hamburg, Germany. (e-mail: feichter@dkrz.de)

W. F. Cooke, Environment Institute, European Commission, I-21020 Ispra, Italy.

(Received November 15, 1995; revised June 3, 1997; accepted June 3, 1997.)